On Subcritical Instability of the Attachment Line Boundary Layer

VASSILIOS THEOFILIS
Department of Applied Mathematics, University of Twente, P.O. Box 217
7500 AE Enschede, The Netherlands

1. Summary

Subcritical instability in the two-dimensional incompressible attachment-line boundary layer remains a topic of debate, after the apparently contradictory results of Hall and Malik (1986) on one hand and Spalart (1988) and Jiménez *et al.* (1990) on the other. Direct Numerical Simulation (DNS) results are presented, aiming at addressing this question. Extensive numerical experimentation has been performed and all results obtained suggest that the two-dimensional model equations describing leading edge boundary layer (LEBL) flow do *not* support solutions growing subcritically in Reynolds number, although the nonlinear neutral loop is seen to bifurcate from its linear counterpart in a manner consistent with the predictions of the theory of Hall and Malik (1986). Nonlinear neutral loops have been obtained suggesting that the two-dimensional model LEBL flow is similar to the classical Blasius boundary layer in terms of the location, in parameter space, of the experimentally observed naturally occuring instability waves.

2. Introduction

The work of Hall *et al.* (1984) established that the eigenvalue problem (EVP) resulting from linear analysis of the generalised Hiemenz (1911) flow (Rosenhead, 1963) adequately predicts the behaviour of small-amplitude disturbances observed experimentally by Pfenninger and Bacon (1969) and Poll (1979). However, LEBL flow may become turbulent at Reynolds numbers well below the linear critical value, $\bar{R} \approx 583$, as observed, f.e., in the systematic experimental studies of Poll (1979, 1985) and three-dimensional DNS of Spalart (1988).

Receptivity being at its early stages of development (Morkovin and Reshotko 1989) deterministic analytical models that may yield predictions for finite-amplitude disturbances pivot about the Stuart-Watson weakly nonlinear analysis (Stuart, 1960; Watson, 1960). Hall and Malik (1986) were the first to apply weakly nonlinear analysis and DNS to the LEBL flow. Their theory predicted that this flow may be potentially destabilised by finite- amplitude disturbances and DNS results obtained by Hall and Malik, on a two-dimensional model, indeed yielded a value of critical $\bar{R} \approx 535$.

Spalart (1988), however, presented DNS results of instability and transition to turbulence without observing, in a number of three-dimensional runs performed, the subcritical behaviour predicted by the Hall and Malik computations. Spalart(1989) used no a-priori assumptions on the form of the perturbations, in contrast with all other work to-date, both theoretical and numerical, which invariably uses the Görtler-Hämmerlin (GH) form (Görtler, 1955; Hämmerlin, 1955). The simulations of Spalart, however, provided evidence that use of this form is permissible.

Jiménez *et al.* (1990) attempted to resolve the issue by considering, numerically, the two- dimensional limit of LEBL flow, since it is on this model that the Hall and Malik theory yields the prediction of (nonlinear) subcritical behaviour in both wave- and Reynolds number. Jiménez *et al.* took the (generalised Hiemenz) stagnation point flow subject to the GH assumption as a model for their base flow and, performing extensive experimentation, concluded that the two- dimensional flow does *not* support subcritical solutions; they suggested that the formally excluded (in view of the GH assumption) three-dimensional mechanisms may be responsible for the observed discrepancy between linear theory and experiment.

Theofilis (1988, 1993) formulated the two- dimensional LEBL flow as an initial-value-problem (IVP) and linearised about the generalised Hie-

Paper presented at the 74th Fluid Dynamics Symposium on "Application of Direct and Large Eddy Simulation to Transition and Turbulence" held at Chania, Crete, Greece, in April 1994.

menz profile using the GH assumption. He obtained results of the IVP that were in line with the EVP predictions of Hall *et al.* (1984). The model problem considered by Theofilis (1988) was shown, in the two-dimensional limit considered, to respond to blowing/suction of the boundary layer in the manner predicted by the EVP in Hall *et al.* (1984) and the three-dimensional DNS of Spalart (1988).

In the present paper we relax the condition of smallness imposed on the perturbations and solve the resulting nonlinear problem. The points on which the numerical procedures utilised herein differ to those presented in Theofilis (1993) are briefly discussed in §3, where an alternative numerical method is presented for the solution of the EVP. In §4 results on the EVP and both the linear and nonlinear IVP are presented. The significance of our nonlinear results with respect to the apparent disagreement between earlier two-dimensional stability results is highlighted. Concluding remarks are offered in §5.

3. Numerical Methods

The governing equations solved are those presented in Theofilis (1993) with the additional inclusion of the nonlinear terms, also presented therein. The temporal model is adopted throughout (Kleiser, 1993); a Fourier expansion is assumed in the homogeneous spanwise direction, treated as periodic, and second-order finite-differences on a stretched grid are used in the normal. The implementation of stretching in the normal direction, as opposed to the uniform grid used in Theofilis (1993), was decided on grounds of efficiency but also in view of the fact that a uniform grid might only be relevant in calculating the late nonlinear stages, which have not been addressed presently. Time-marching is performed by an implicit Crank-Nicolson scheme in view of (a) its stability properties and (b) the relatively short integration times in the present study. Further technical details may be found in Duck (1985) and Theofilis (1993).

The forcing of the simulations is provided by choosing the wall normal perturbation velocity in spectral space to be a smootlhy varying function of space and time. We have focussed on two forms of forcing, one jet-like, and one simulating ribbon excitation. The forms of these functions are given explicitly in Theofilis (1993). The former is a short-lived function of space and time while the latter is a function with a parametric dependence on the frequency of the maximally amplified linear mode. It should be mentioned here that the terms *jet* and, especially, *ribbon* are used to provide only qualitative description. Comparison of simulation results with experiments whose excitation is provided by, say, a vibrating ribbon, require the former to adopt the spatial model and three-dimensional calculations. Neither of the two falls into the scope of the present study.

Information on the EVP is desired for the nonlinear computations. It was thought appropriate to obtain this information by a numerical approach independent of that utilised for the simulations. The EVP system, of the Orr-Sommerfeld class, but *not* the Orr-Sommerfel equation (Poll, 1978; Arnal, 1992; Theofilis, 1994) is thus solved using spectral collocation based on Chebyshev polynomials. Of the results obtained the growth rate has been utilised to perform comparisons with those yielded by the IVP approach and the frequencies in order to force some of the nonlinear calculations described in the sequel.

4. Results

Results obtained may be classified as follows. Firstly, as mentioned, EVP results. Subsequently, linear IVP results which, when compared to the EVP results, provide validation of the IVP numerical approach. Finally, nonlinear results; the latter have been obtained under the two distinct forms of the forcing function discussed earlier. The amplitude of the forcing function was utilised as a parameter to control the size of the disturbances initially introduced into the numerical solution.

4.1. The Eigenproblem Revisited

Spectral collocation was selected to solve the eigenvalue problem in view of the favourable accuracy properties of spectral methods for smooth functions (Canuto *et al.* 1993). Within the context of collocation calculations Chebyshev polynomials were preferred to other spectral basis functions, based on arguments related to the minimax property of Clyebyshev polynomials used in conjunction with the standard Gauss and Gauss-Lobatto grids (Boyd, 1989). The grid refinement history at the neutral conditions (zero suction) $\bar{R} = 800, \beta = .3384638$ quoted by Hall *et al.* (1984) is presented in Table I.

Utilising $N = 160$ points, compact finite-differences, and asymptotic boundary conditions, Hall *et al.* (1984) predict that the neutral mode at

these conditions has a frequency $c_r = 0.3755134$.

N	c_r	c_i
16	0.3881956	-.0010554
32	0.3754382	-.0000697
64	0.3755143	-.0000007

TABLE I
Grid refinement history in our spectral collocation numerical solution of the EVP at $\bar{R} = 800, \beta = .3384638$.

It may be seen from the results of Table I that $N = 64$ collocation nodes suffice in order to produce converged EVP results. The smaller number of nodes utilised compared to compact finite-differences results in substantial savings when using the QZ algorithm (Wilkinson, 1965; NAG, 1992) to solve the eigenproblem.

Moreover, our results are obtained on a large (one-dimensional) integration domain, at both endpoints of which we impose the boundary condition of vanishing perturbations. This condition is more general than the prespecified exponential decay prescribed by Hall *et al.* (1994); the identical results obtained, however, justify use of the asymptotic behaviour of the perturbations assumed by Hall *et al.* (1994).

4.2. An IVP Formulation: Linear

In the IVP formulation of the stability problem we assume the decomposition of all flow quantities into base and perturbed flow. In the linear regime we expect the perturbations to be small compared to the $O(1)$ base flow and set quadratic in perturbations terms to be identically equal to zero. We subsequently march the solution in time and monitor the behaviour of the perturbed flow.

We utilise the jet-like excitation and obtain results typical examples of which are presented in figures 1 and 2 where the time dependence of the wall shear component in the streamwise direction u_y of an (almost) neutral and a decaying mode is plotted. After some transient, Tollmien-Schlichting (TS) waves emerge, whose growth or decay in time depends upon the combination of the Reynolds number and wavenumber parameter values.

The growth rate of an individual TS mode may be monitored in either real or transform space; the simulation is terminated when convergence of the growth rate has been achieved. The growth rate dependence on time for the results of figures 1 and 2 is also presented. The frequency of a TS mode is another result that may be directly calculated from the numerically obtained IVP linear results. Both frequency and growth rate linear results have been compared against the results of Hall *et al.* (1984) and those obtained by our collocation EVP approach with very good agreement resulting.

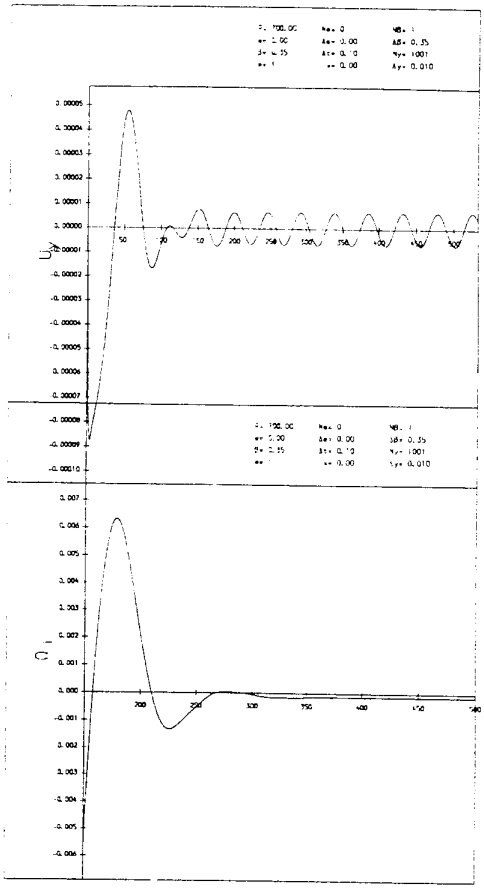

Fig. 1. An almost neutral linear TS mode at $\bar{R} = 700$, spanwise wavenumber $\beta = 0.35$. Upper: wall shear u_y against time t. Lower: growth rate ω_i against time t.

4.3. An IVP Formulation: Nonlinear

The smallness condition of the perturbed flow quantities is next relaxed and the resulting nonlinear system is solved numerically. We concentrate on the zero suction case and define our integration box according to the following criteria. In the wall-normal we truncate the domain at a distance large enough for imposition of the

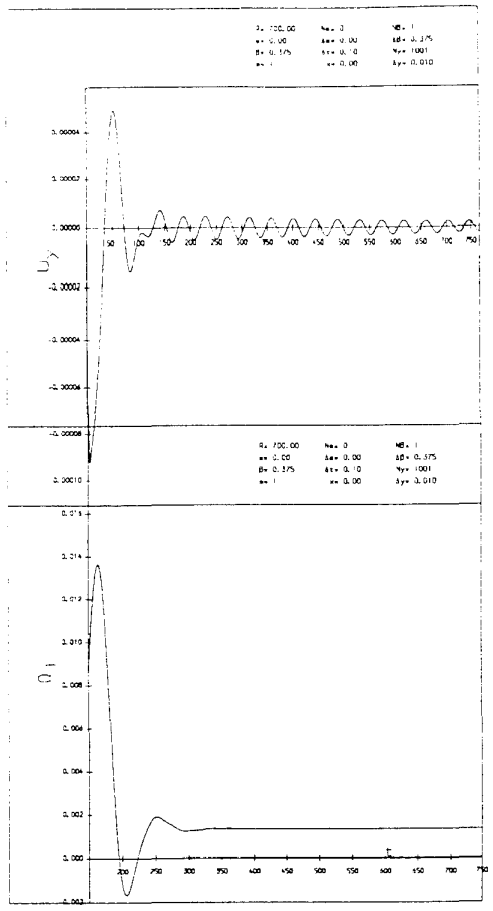

Fig. 2. A decaying linear TS mode at $\bar{R} = 700$, spanwise wavenumber $\beta = 0.375$. Upper: wall shear u_y against time t. Lower: growth rate ω_i against time t.

boundary condition of zero perturbations to be applicable. The reason for this choice is, again, our unwillingness to introduce an a-priori free-stream rate of decay on the perturbations. A large number of nodes, typically of $O(200)$ are taken in this direction in view of the extent of the domain and the low accuracy of the numerical method in this direction. In the spanwise direction a modest-to-large number of Fourier nodes, typically $O(100)$, may be devoted to either fine resolution of the fundamental or capturing of a number of subharmonics. In this study we have chosen the first course of action, concentrating on the domain suggested by the linear response.

Similarly to the linear IVP results, instability waves develop in the flow after some transient; a typical example is shown in figure 3. Values of the growth rate, ω_i, are calculated either through

$$\omega_i = \frac{1}{\hat{\phi}} \frac{d\hat{\phi}}{dt} \tag{1}$$

using the time signal of a spectral space flow quantity $\hat{\phi}$ (harmonic of the respective physical space quantity) or, equivalently, through monitoring a measure of the perturbation energy

$$E(\beta, t) = \int_0^{y_\infty} \{\hat{u}^2 + \hat{v}^2 + \hat{w}^2\} dy \tag{2}$$

$\hat{u}, \hat{v}$ and $\hat{w}$ indicating, respectively, perturbation velocity components in the streamwise, normal and spanwise directions, and calculating the slope of the function

$$\ln \sqrt{E(t)} \tag{3}$$

at a given wavenumber β value. The two definitions yield identical results.

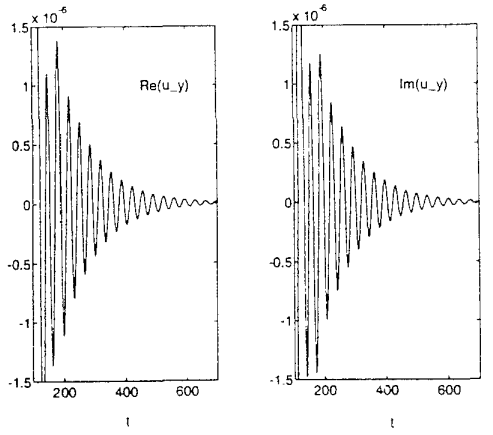

Fig. 3. Wave emerging at $\bar{R} = 550, \beta = 0.3$. Left: $\Re\{u_y\}$ against time. Right: $\Im\{u_y\}$ against time.

The quantity defined in (2) is, additionally, significant in that it measures the strength of an individual Fourier component and, as such, may be monitored in relation to resolution requirements of the simulation (Reed, 1993). Such a study has been performed in the course of the runs presented and a typical result is plotted in figure 4. Worth noticing here are, firstly, that the typical of spectral simulations linear dependence of the logarithm of energy on the number of nodes utilised is clearly exhibited. Secondly, it has been demonstrated (f.e. Zang *et al.*, 1989) that a minimum requirement for reliability of results obtained in transition simulation is the separation of the energy of the most-from the least-energetic (Fourier) modes by at least eight orders of magnitude; more than ten orders of magnitude separation is demonstrated

in figure 4. Moreover, the typical tail in the energy spectrum which denotes imminent loss of accuracy due to accumulation of energy in high-wavenumbers is absent from our calculations.

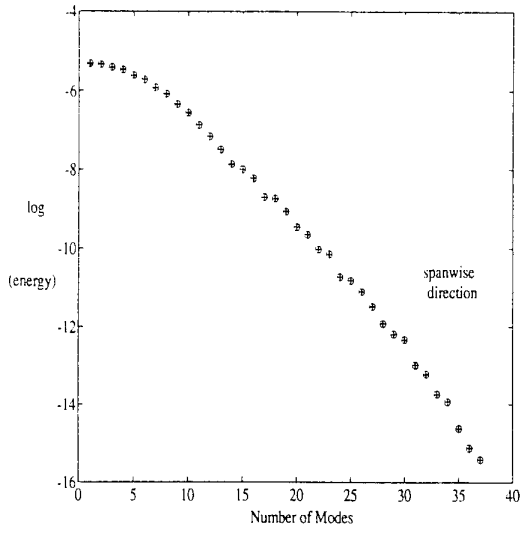

Fig. 4. Spanwise resolution quality test.

The issue of the link between resolution and de-aliasing has also been considered in the present nonlinear calculations. It was found to be irrelevant to actually invoke the dealiasing option in conjunction with the high resolutions utilised, although it was necessary to de-aliase our calculations during runs on more modest grids. This result appears to be in line with the emerging consensus that de-aliasing may be relevant for marginally resolved simulations (Spalart *et al.* 1991; Canuto *et al.* 1993). For the two-dimensional results presented herein, however, it is straightforward to resolve all scales at the early nonlinear stages considered.

We first compare our nonlinear IVP calculations against those yielded by the linear IVP approach. In figures 5 and 6 we present such a typical comparison between linear and nonlinear IVP results, the latter obtained under linear conditions, at a given set of parameters. Though undergoing different transient behaviour, the two sets of calculations yield, at convergence, identical frequency and growth rate results.

We next turn to nonlinear calculations and present in figure 7 a typical dependence of the perturbation energy function defined in (3) on the spanwise wavenumber and time at a given Reynolds number. This function becomes a linear function of time at a given wavenumber after some initial transient, indicating the onset of flow behaviour described by linear theory. The sign of the slope of an individual straight line determines growth or decay of the respective instability wave. Interpolation of the results at different wavenumbers determines the location in parameter space of the branches of the neutral loop. Repeating similar calculations at different Reynolds number values one obtains a complete (nonlinear) neutral loop.

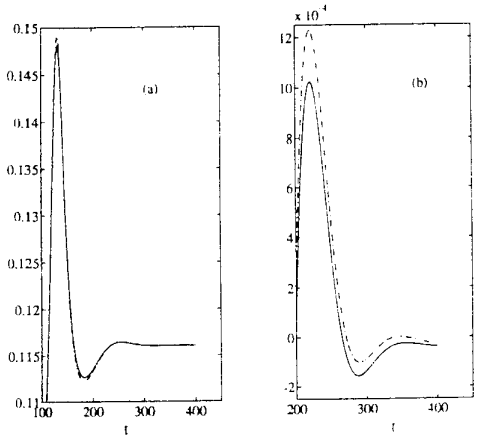

Fig. 5. Frequency in(a) and growth rate in(b) against time at $\bar{R} = 590$, spanwise wavenumber $\beta = 0.3$ predicted by linear and nonlinear numerical solution.

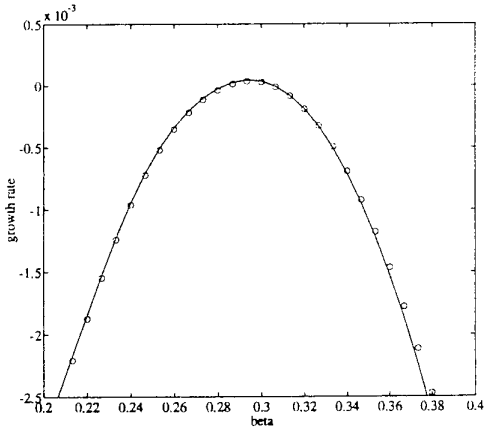

Fig. 6. Linear and nonlinear growth rate vs. wavenumber at $\bar{R} = 590$.

In order to address the issue of existence of two-dimensional nonlinear subcritical solutions we first obtain nonlinear solutions under linear conditions, namely small amplitude of the initially superimposed disturbance. Utilising the jet-like excitation we have scanned the Reynolds number parameter range in the neighbourhood of the neutral loop that linear theory delivers; all our results have been qualitatively similar to those

presented in figures 5 and 6, namely the flow returns to its linear behaviour after the initial transient.

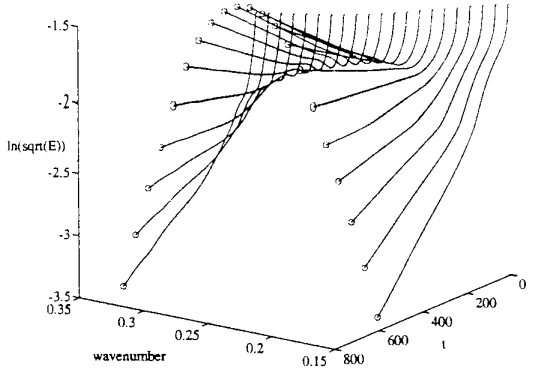

Fig. 7. Perturbation energy as function of time at $\bar{R} = 800, \beta \in [0.15, 0.35]$.

We then concentrate on a single Reynolds number value $\bar{R}$=550, which is approximately located in the middle of the disputed region and, keeping all other parameters the same, alter the form of the forcing. We consider the ribbon-like excitation which we apply for a number of TS cycles before abruptly removing it. We introduce periodic suction and blowing into the numerical solution choosing the frequency of the ribbon operation to be that of the most unstable (decaying) linear mode at the given Reynolds number value.[1] The result is presented in figure 8 from which two conclusions may be drawn. Firstly it may be seen that the ribbon sets up a (forced) neutral oscillation. Secondly, once the forcing is removed, the flow returns to its linear behaviour, namely (strongly) decaying oscillation. Incidentally it is worth noting that, although a sharp peak follows the removal of the forcing at $t = 750$, there is no lasting effect on the simulation stemming from this singular alteration in boundary conditions.

Keeping the same Reynolds number value and reverting to the jet-like excitation we progressivley increase the amplitude of the initially imposed perturbation. The effect of this action, as may be seen from the result presented in figure 9, is that a longer transient ensues in the nonlinear solution. In the course of this transient behaviour solutions corresponding to large initial excitation amplitudes spend time grow-

[1] This frequency was independently obtained from the EVP problem discussed in §3.1

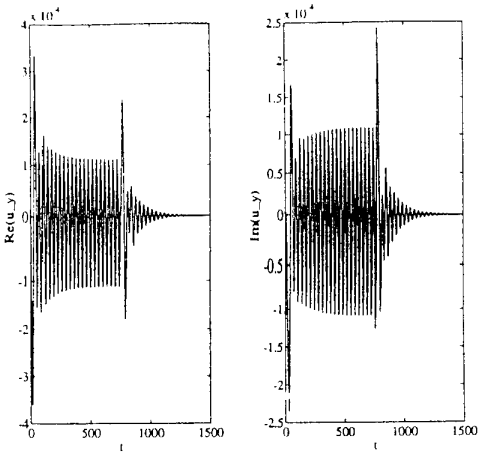

Fig. 8. Wall shear u_y dependence on time t using the ribbon-like forcing at $\bar{R} = 550$: initially a neutral wave of the imposed frequency is generated; after the forcing is being removed a decaying wave emerges.

ing while their linear counterparts (the solutions which correspond to the lowest initial excitation amplitude) have long converged to their decaying state. However, this behaviour of the former solutions is only transient; eventually all calculations are seen to fall back to the linear result.

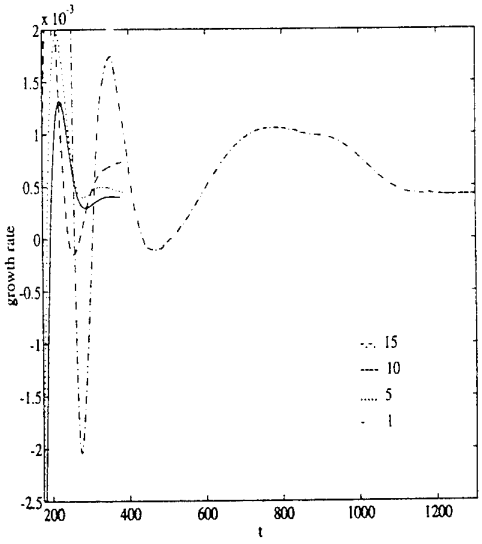

Fig. 9. Growth rates time history for increasing initial excitation amplitudes ε: Solid, $\varepsilon = 1$ (linear result); dashed, $\varepsilon = 5$; dash-dotted, $\varepsilon = 10$; dotted, $\varepsilon = 15$.

In the neighbourhood of the linear neutral loop, however, nonlinear solutions have been obtained that bifurcate (to different degrees) from the linear loop. A typical example is presented in figure 10 where the modal perturbation energy and respective growth rates of linear and nonlin-

ear computations are plotted against time at spanwise wavenumber increments of $\Delta\beta = 0.01$. This result is obtained at conditions favouring linear growth ($\bar{R} = 800$, in the neighbourhood of Branch I) utilising the jet-like form of forcing and a large initial excitation amplitude.

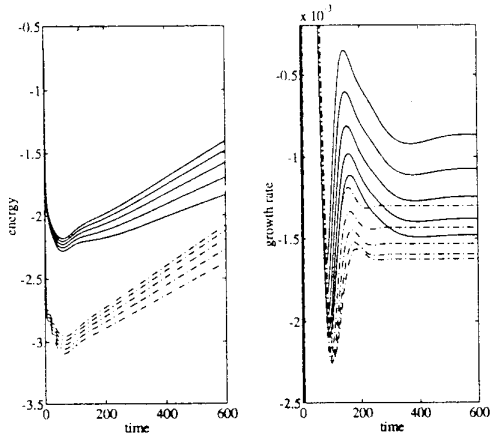

Fig. 10. Nonlinear (solid) vs. linear (dashed) results at $\bar{R} = 800$. Lower to higher: spanwise wavenumber $\beta = 0.15(.01)0.19$.

The growth rate dependence on wavenumber for both linear and nonlinear calculations is presented in figure 11; projected in figure 11 are also the (linearly interpolated) linear and nonlinear neutral loops, as well as the line of maximum amplification rate of the nonlinear calculation. Three results of significance may be observed in this figure.

Firstly, as may already be inferred from the results of figure 10, the nonlinear neutral loop is confined in a thin region around the linear loop. This result is similar to that obtained by Jiménez *et al.* (1990) and appears to support the theoretical prediction of Hall and Malik (1986).

Secondly, the consequence of the departure of the nonlinear neutral loop from the linear result is that the maximum amplification rate of the nonlinear neutral curve lies very close to the experimentally observed waves (c.f. Pfenninger and Bacon, 1969; Poll, 1979). To-date it has been assumed that the experimentally observed naturally occurring waves are Branch I instabilities. It is well known, however, that naturally occurring disturbances in Blasius flow peak near the theoretical maximum amplification and maximum amplitude ratio curves (see f.e. Poll, 1989). The present results appear to yield such a behaviour for the LEBL flow as well.

Finally, one may notice that the dependence of the maximum amplification rate on Reynolds number is very similar between the linear and nonlinear results. One may infer from the results presented in figure 11 that, in contrast with the numerical predictions of Hall and Malik (1986) and in line with a similar result of Jiménez *et al.* (1990), our nonlinear calculations on the present two-dimensional model yield a critical Reynolds number value close to that delivered by linear theory.

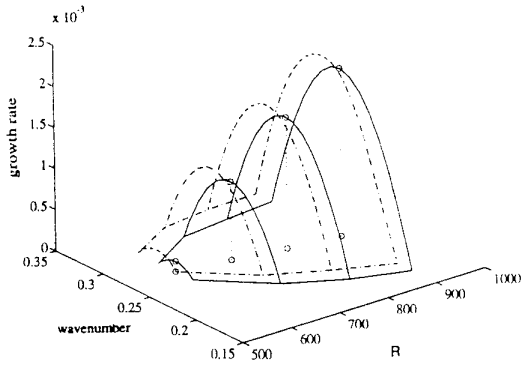

Fig. 11. Linear vs Nonlinear neutral loops; projected the line of maximum amplification rate.

5. Discussion

An effort has been made to address the issue of subcritical behaviour in incompressible two-dimensional attachment line flow. The initial-value-problem approach for the linear stability problem of Theofilis (1993) has been extended to allow for more general forms of perturbations, in an attempt to systematically relax the approximations under which the stability of incompressible leading edge boundary layer flow is studied.

In line with the numerical work of Jiménez *et al.* (1990) and contrary to the numerical conclusions put forward by Hall and Malik (1986), we failed to observe nonlinear solutions bifurcating subcritically in Reynolds number. The argument put forward by Spalart (1988) on the inability to draw conclusions on analytical models by a limited number of numerical runs still holds. However, the extent of the numerical experimentation performed on the two-dimensional model

considered presently appears to support the conclusion of Jiménez *et al.* (1990) that three-dimensional mechanisms are to be held responsible for the experimentally observed subcriticality.

The present nonlinear calculations have yielded neutral loops the location of which, in parameter space, suggests that the experimentally observed instability waves occur at (approximately) maximally amplified, rather than Branch I conditions. While work is in progress to quantify this conjecture, this result suggests that the attachment line boundary layer is, in this respect, akin to the classical Blasius flow.

References

1. Arnal, D., (1992). Boundary Layer Transition: Prediction, Application to Drag Reduction. *AGARD Rep. 786*, p.5-1.
2. Boyd, J. P., (1989). *Chebyshev and Fourier Spectral Methods*, Lecture Notes in Engineering **49**, Springer.
3. Canuto, C., Hussaini, M. Y., Quarteroni, A. and Zang, T. A., (1987). *Spectral Methods in Fluid Dynamics*, Springer Verlag, Berlin.
4. Duck, P. W., (1985). *J. Fluid Mech.* 160, p.465.
5. Görtler, H., (1955). Dreidimensionale Instabilität der ebenen Staupunktströmung gegenüber wirbelartigen Störungen. in *50 Jahre Grenzschichtforschung*, (H. Görtler & W. Tollmien eds.), p.304, Vieweg und Sohn, Braunschweig.
6. Hämmerlin G., (1955). Zur instabilitätstheorie der ebenen Staupunktströmung. in *50 Jahre Grenzschichtforschung*, (H. Görtler & W. Tollmien eds.), p.315, Vieweg und Sohn, Braunschweig.
7. Hall, P. and Malik, M. R., (1986). On the instability of a three-dimensional attachment-line boundary layer: weakly nonlinear theory and a numerical approach. *J. Fluid Mech.* , **163**, p.257.
8. Hall, P., Malik, M. R. and Poll, D. I. A., (1984). On the Stability of an Infinite Swept Attachment-Line Boundary Layer. *Proc. Roy. Soc.* **A 395**, p.229.
9. Hiemenz, K., (1911). *Dingl. Polytechn. J.* **326**, p.321.
10. Jiménez, J., Martel, C., Agüi, J. C. and Zufiria, J. A., (1990). Direct numerical simulation of transition in the incompressible leading edge boundary layer. *Techn. Note ETSIA* **MF-903**.
11. Kleiser, L., (1993). AGARD-FDP-VKI LS-06: *Progress in Transition Modelling*, VKI, Brussels, Belgium, March 29 - April 1.
12. Morkovin, M. V., and Reshotko, E., (1989). in I.U.T.A.M. SYMPOSIUM ON TRANSITION AND TURBULENCE, III, Toulouse, Springer Verlag.
13. NAG, (1992). Numerical Algorithms Group, *Mark 15*.
14. Pfenninger, W., and Bacon, J. W., (1969). Amplified laminar boundary layer oscillations and transition at the front of a 45° swept flat-nosed wing with and without boundary layer suction. in *Viscous Drag Reduction*, (C. S. Wells ed.), Plenum Press, p.85.
15. Poll, D. I. A., (1978). *College of Aeronautics* Rep. **7805**.
16. Poll, D. I. A., (1979). Transition in the infinite swept attachment line boundary layer. *The Aeronautical Quart.* **30**, p.607.
17. Poll, D. I. A., (1985). *J. Fluid Mech.* 150, p.329.
18. Poll, D. I. A., (1989). in *Computational Methods in Aeronautical Fluid Dynamics*, (P. Stow ed.), Oxford University Press, p.171.
19. Reed, H. L., (1993). AGARD-FDP-VKI LS-06: *Progress in Transition Modelling*, VKI, Brussels, Belgium, March 29 - April 1.
20. Rosenhead, L., (1963). *Laminar Boundary Layers*, Oxford University Press.
21. Spalart, P. R., (1988). Direct Numerical Study of Leading-Edge Contamination. *AGARD CP-438*, p.5-1.
22. Spalart, P. R., Moser, R. D., and Rogers, M. M. (1991). Spectral methods for the Navier-Stokes equations with one infinite and two periodic directions. *J. Comp. Phys.* **96**, pp. 297-324.
23. Stuart, J. T., (1960). *J. Fluid Mech.*, 9, p.352.
24. Theofilis, V., (1988). *M.Sc. Thesis*, Dept. of Mathematics, University of Manchester.
25. Theofilis, V., (1993). Numerical Experiments on the Stability of Leading Edge Boundary Layer Flow: A Two-Dimensional Study. *Int. J. Numer. Methods Fluids*, **16**, p.153.
26. Theofilis, V., (1994). The Discrete Temporal Eigenvalue Spectrum of the Generalized Hiemenz Boundary Layer Flow as Solution of the Orr-Sommerfeld Equation., *Journal Eng. Math.* , (to appear in Vol. **28**).
27. Watson, J., (1960). *J. Fluid Mech.*, 9, p.371.
28. Wilkinson, J. H., (1965). *The Algebraic Eigenvalue Problem*, Clarendon.
29. Zang, T. A., Krist, S. E., and Hussaini, M. Y., (1989). *J. Sci. Comp.*, **4**, vol. 2, pp.197-217.